

## Machine Learning

Zitierweise: *Angew. Chem. Int. Ed.* **2021**, 60, 24354–24366

Internationale Ausgabe: doi.org/10.1002/anie.202107369

Deutsche Ausgabe: doi.org/10.1002/ange.202107369

# Applying Machine Learning to Rechargeable Batteries: From the Microscale to the Macroscale

*Xiang Chen, Xinyan Liu, Xin Shen and Qiang Zhang\****Stichwörter:**

battery lifespan prediction ·  
fast-charge optimization ·  
machine learning ·  
multiscale simulations ·  
rechargeable  
batteries



**E**merging machine learning (ML) methods are widely applied in chemistry and materials science studies and have led to a focus on data-driven research. This Minireview summarizes the application of ML to rechargeable batteries, from the microscale to the macroscale. Specifically, ML offers a strategy to explore new functionals for density functional theory calculations and new potentials for molecular dynamics simulations, which are expected to significantly enhance the challenging descriptions of interfaces and amorphous structures. ML also possesses a great potential to mine and unveil valuable information from both experimental and theoretical datasets. A quantitative “structure–function” correlation can thus be established, which can be used to predict the ionic conductivity of solids as well as the battery lifespan. ML also exhibits great advantages in strategy optimization, such as fast-charge procedures. The future combination of multiscale simulations, experiments, and ML is also discussed and the role of humans in data-driven research is highlighted.

## 1. Introduction

To mitigate the acceleration of global warming, achieving a zero net carbon dioxide emission has become a goal with international consensus, which requires the reconstruction of energy storage systems for all types of usage. Reducing the consumption of routine fossil fuels such as coal, oil, and gas, as well as increasing the usage of renewable energy, such as wind and solar energy, are in high demand to establish a green and sustainable energy system. Consequently, advanced energy storage technology plays an unprecedented role because of the wide distribution and intermittency of renewable energy. Energy storage devices are expected to bridge the requirements of renewable energy and the energy demands of human daily life and industry.<sup>[1,2]</sup>

As a typical energy storage device, the lithium (Li) ion battery (LIB) has been used in a wide range of applications—from portable electronics to electric vehicles and even large-scale smart grids.<sup>[2,3]</sup> To further increase the consumption percentage of renewable energy, the development of advanced batteries with high energy densities, high power densities, long lifespans, and reliable safety is deemed essential and also the ultimate goal of the energy community. Beyond conventional LIBs, lithium metal batteries (LMBs), including lithium–sulfur (Li–S) batteries and solid-state batteries, emerge as promising candidates for the next-generation energy storage devices because of their ultrahigh energy densities.<sup>[4–6]</sup>


Despite their promising energy densities, the practical application of LMBs faces huge challenges, including the limited fundamental understanding of the battery working mechanisms, the lack of rational design guidelines for advanced electrodes and electrolytes, and the extremely high requirements for the packing technology.<sup>[5,7,8]</sup> Unlike routine LIBs that are based on the Li<sup>+</sup> intercalation mechanism, LMBs are based on conversion reactions, and complicated multiphase reactions are typically involved. The large struc-

tural change of the electrode material and interface subsequently induces a rapid degradation of the capacity and even causes safety hazards. Although great progress has been made both experimentally and theoretically with LMBs,<sup>[8,9]</sup> it is still a great challenge to rationally construct a safe and high-performance LMB and efficiently monitor its working state. Experimental tests, including long-term cycling and rate capability, are widely adopted to evaluate the electrochemical performance of a functional material or recipe. However, it is almost impossible to optimize the battery performance in a short time through a mere trial-and-error approach due to the abundance in the material and component space. Various characterization techniques such as scanning electron microscopy (SEM), transmission elec-

tron microscopy (TEM), and X-ray photoelectron spectroscopy, are often employed to probe the working mechanism or chemistry of a material or method. However, in situ characterization at the atomic level is very limited, which makes the discovery of structure–function relationships and obtaining a fundamental understanding of the working mechanism extremely challenging. On the other hand, computational chemistry and materials methods—especially density functional theory (DFT) calculations and molecular dynamics (MD) simulations—are widely applied in research on rechargeable batteries<sup>[6,10,11]</sup> and have afforded fruitful insights into the molecular interaction,<sup>[10,12]</sup> interfacial reactions,<sup>[13,14]</sup> and ionic transport mechanism.<sup>[15]</sup> However, routine theoretical studies often face great obstacles as the system size or the required accuracy grows. The gap between simplified theoretical models and reality largely impedes the application of computational simulations to describe complicated interfacial problems in batteries, such as the solid electrolyte interphase (SEI), the thermodynamics and kinetics of lithium polysulfide conversion reactions, the electrolyte solvation structure at electrode interfaces, and the ionic transport behavior at the liquid–solid or solid–solid interfaces.

Recently, emerging machine learning (ML) technology has brought new opportunities for both theoretical and experimental studies in chemistry and materials science.<sup>[16,17]</sup>

[\*] Dr. X. Chen, Dr. X. Liu, X. Shen, Prof. Q. Zhang  
Beijing Key Laboratory of Green Chemical Reaction Engineering and Technology  
Department of Chemical Engineering  
Tsinghua University, Beijing 100084 (China)  
E-Mail: zhang-qiang@mails.tsinghua.edu.cn  
Dr. X. Liu  
Institute of Fundamental and Frontier Sciences  
University of Electronic Science and Technology of China  
Chengdu 611731, Sichuan (China)

 The ORCID identification number for the authors of this article can be found under: <https://doi.org/10.1002/anie.202107369>.



ML methods are expected to accelerate the development of theoretical methods (e.g. developing new functionals<sup>[18,19]</sup> or potential functions<sup>[20–22]</sup>) so that larger systems can be handled with higher accuracy. The structure–function relationship of a complicated system can, therefore, be discovered and unveiled more efficiently. More importantly, a novel research approach has been established based on ML methods. This statistically driven design is completely different from conventional theoretical approaches, which mainly involve structure–property calculations or crystal structure prediction.<sup>[23]</sup> The numerous datasets generated through high-throughput calculations and experiments are fed into ML to discover valuable information and hidden correlations, which can be quite challenging in current physical science. Based on high-quality datasets, the ML models have been shown to have the ability to predict the physicochemical properties of materials (such as ionic conductivity and viscosity<sup>[24]</sup>) and assist the design of functional materials (such as drugs,<sup>[25,26]</sup> energy materials,<sup>[27,28]</sup> porous materials,<sup>[29]</sup> and small molecules<sup>[30]</sup>). Consequently, experimental, theoretical, and data tools have become three indispensable methods in current scientific research and are displaying great potential in battery studies (Figure 1).

In this Minireview, we focus on the application of machine learning to advanced rechargeable batteries—from the microscale to the mesoscale and finally to the macroscale. The cooperation between ML and various theoretical or experimental methods, such as DFT calculations, MD simulations, the phase field method (PFM), the finite element method (FEM), battery material characterization techniques, and electrochemical performance tests are elaborated. Finally, an outlook on how to combine experiments, theory, and machine learning to promote the practical application of next-generation batteries is provided.

## 2. An Overview on Machine Learning at Different Time and Length Scales

Machine learning is a branch of artificial intelligence and a method of data analysis that can learn from data, identify patterns, and make decisions with minimal human intervention. Driven by the rapid growth of data storage and related computer science techniques, machine learning has blossomed in recent years and has achieved wide applications, such as in the computer sciences (e.g. image recognition), chemis-

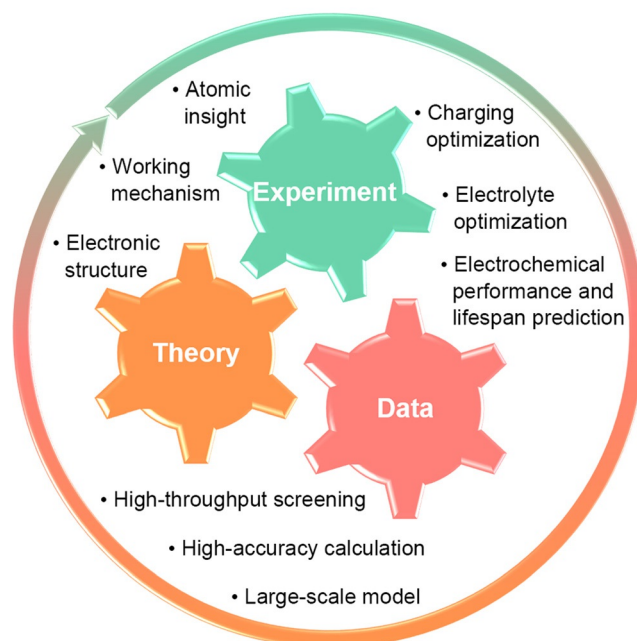


**Figure 1.** Three approaches in battery studies, including experimental, theoretical, and data tools.

try and materials sciences (e.g. property prediction, materials design), social media (e.g. production recommendation), and even humanities and social sciences (e.g. automatic language translation, paper reading). Data can be generated much more easily from both experiments and theoretical calculations, whereas mining all the valuable information and hidden correlations behind the data by conventional approaches poses a tremendous challenge. Therefore, a variety of ML methods have been developed, including the Bayesian network, decision tree, artificial neural network (ANN), and support vector machines (Figure 2).<sup>[25]</sup> The fundamentals of these ML methods have been summarized well in many great reviews,<sup>[25,28,29,31]</sup> and we hereby focus mainly on the applications of ML to battery research.

Rechargeable batteries are generally composed of anodes, cathodes, electrolytes, separators, current collectors, and packing materials, and each component often consists of several materials. For example, the electrolyte used in commercial LIBs includes nearly 20 kinds of solvents, lithium salts, or additives.<sup>[32]</sup> Therefore, battery studies involve various multidisciplinary scientific problems and are faced



Xiang Chen gained his bachelor degree and PhD with Prof. Qiang Zhang from the Department of Chemical Engineering at Tsinghua University in 2016 and 2021, respectively. He is currently a postdoctoral fellow at Tsinghua University with Prof. Qiang Zhang. His research interests focus on understanding the chemical mechanism and materials science of rechargeable batteries through multiscale simulations and machine learning.



Qiang Zhang received his bachelor degree and PhD with Prof. Fei Wei from Tsinghua University in 2004 and 2009, respectively. After research at Case Western Reserve University (USA) with Prof. Liming Dai and at the Fritz Haber Institute of the Max Planck Society (Germany) with Profs. Robert Schlögl and Dangsheng Su, he joined the faculty of Tsinghua University in 2011. His current research interests are advanced energy materials, including Li metal anodes, solid-state electrolytes, Li–S batteries, and electrocatalysts.

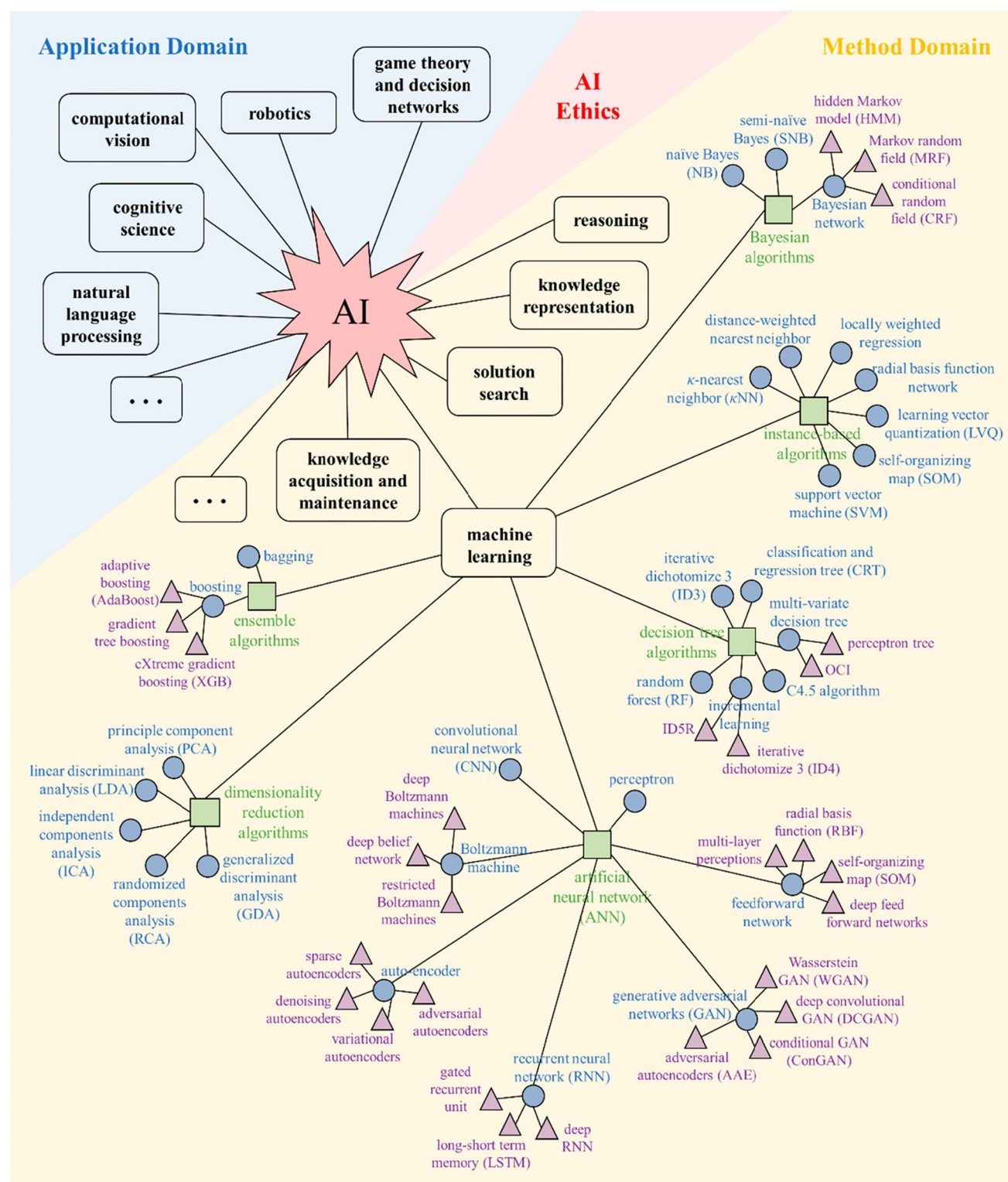


**Figure 2.** Summary of typical machine learning and artificial intelligence techniques. Reproduced with permission.<sup>[25]</sup> Copyright 2019, American Chemical Society.

with numerous engineering challenges from the microscale to the macroscale. The research methods vary on different length scales, including on the atom/molecule, cluster/crystal, particle, electrode, cell, and finally pack (Figure 3). Not only does ML exhibit great advantages for analyzing the large

datasets generated and establishing quantitative relationships for the rational design of a material or method, it also plays an increasingly nontrivial role in promoting the development of theoretical and experimental methods, such as the functionals in DFT calculations and the interatomic potentials in MD

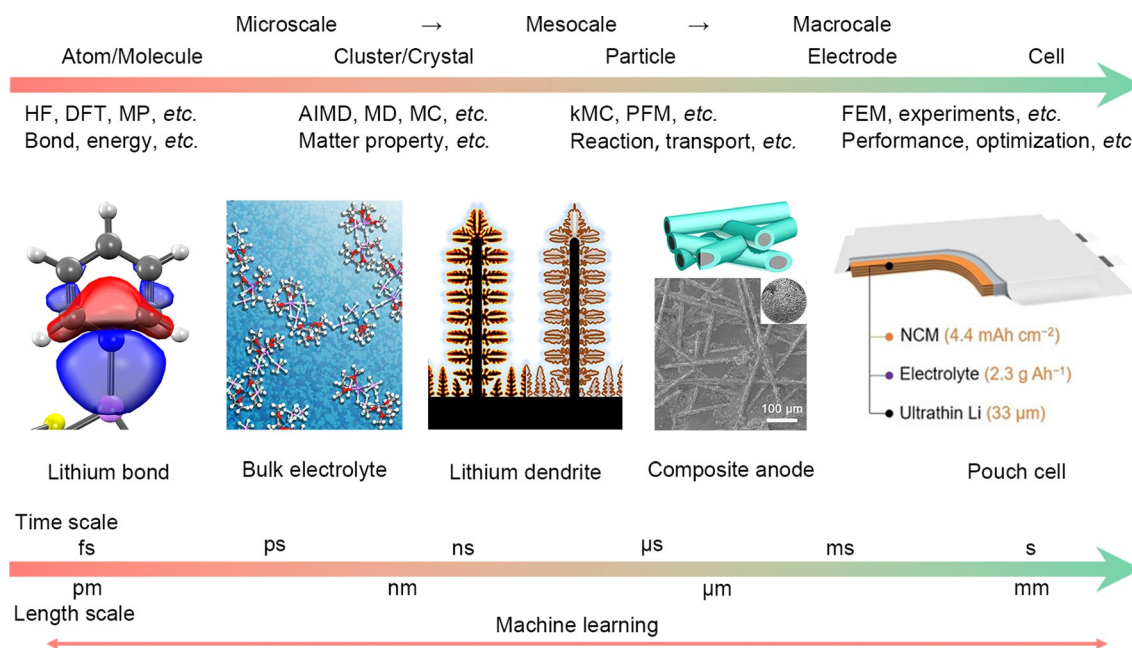


**Figure 3.** The application of machine learning in battery research at different length and time scales. HF: Hartree–Fock, DFT: density functional theory, MP: Møller–Plesset perturbation theory, AIMD: ab initio molecular dynamics, MD: molecular dynamics, MC: Monte Carlo, kMC: kinetic Monte Carlo, PFM: phase field method, and FEM: finite element method. The inserted figures were obtained from previous reports. Reproduced with permission.<sup>[35–37]</sup> Copyright 2017, Wiley-VCH; Copyright 2020, Elsevier; Copyright 2019, Elsevier; Copyright 2018, Elsevier, and Copyright 2017, Elsevier, respectively.

simulations. The ML models are expected to speed up conventional high-accuracy calculations for large systems. For example, MD simulations of 100 million atoms with ab initio accuracy have been achieved by a deep-learning potential approach.<sup>[33,34]</sup>

classified into two categories: developing novel ML-assisted DFT/MD methods and making predictions based on DFT/MD results (Figure 4). The former aims to obtain energetic and force-related information with reduced computational cost, while the main target of the latter is directly predicting properties of interest in the system.

### 3. Microscale and Mesoscale Simulations

#### 3.1. DFT Calculations and MD Simulations

Computational methods are extremely powerful and effective for obtaining the electronic and geometric structure, total energy, dipole moment, and charge distribution of molecules or crystals. Specifically, DFT calculations and MD simulations are widely employed in battery studies and have led to some great success with experimental verifications, such as designing functional hosts to mitigate the shuttling of lithium polysulfides in Li–S batteries,<sup>[38]</sup> probing electrolyte solvation structure and redox stability,<sup>[12,14,36,39]</sup> and unraveling the ionic transport mechanism in solid electrolytes.<sup>[40]</sup> The application of ML to DFT calculations or MD simulations can be

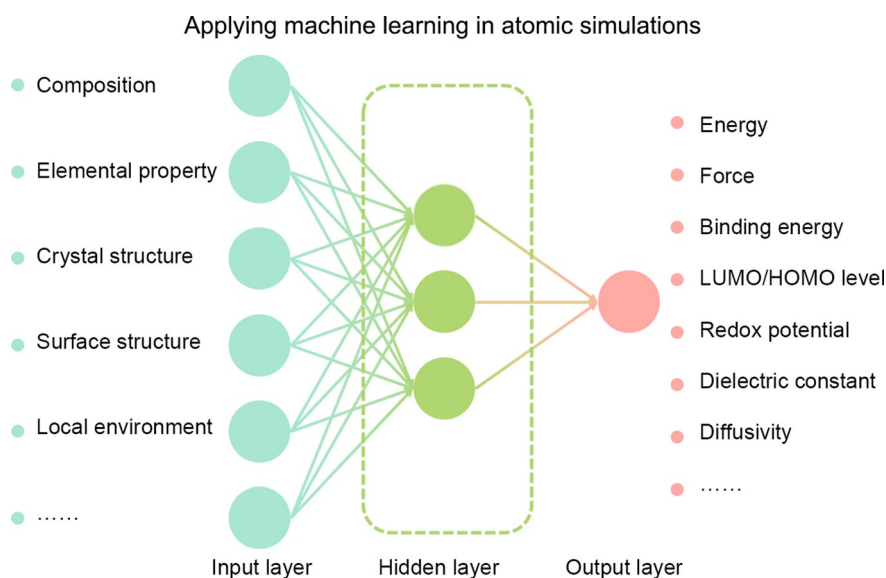


**Figure 4.** Correlating material parameters and physicochemical properties through machine-learning approaches. LUMO: lowest unoccupied molecular orbital, HOMO: highest occupied molecular orbital.



The accuracy and speed of DFT calculations are usually inversely correlated, which remains one of the major obstacles when applying DFT calculations in large-scale models. Emerging functionals, such as SCAN (strongly constrained and appropriately normed),<sup>[41]</sup> has been shown to match or even improve the accuracy of a computationally intensive hybrid functional at almost GGA (generalized gradient approximations) cost. More importantly, ML brings new possibilities to speeding up the development of novel functionals through training accurate exchange and correlation functionals based on the electronic density.<sup>[18]</sup> Apart from accelerating the development of the functionals, ML also shows superior performance in determining the Hubbard  $U$  parameter in DFT +  $U$  calculations compared to the conventional linear response approach.<sup>[42]</sup> Therefore, ML methods are expected to improve the efficiencies and accuracies of DFT calculations.

Not only does machine learning help to make DFT more powerful, it also supplies a completely innovative perspective to analyze the DFT calculations. The total energy of the system is one of the most basic types of information obtained from DFT calculations, from which many key physicochemical parameters, such as binding energy, redox potential, and diffusion barrier, can be derived. It is, therefore, quite convenient to construct a large dataset containing the energetic information of a class of functional materials by DFT calculations, where ML models can then be adopted to construct a scaling relationship between the structural and energetic properties of the materials. This scheme is widely applied in designing electrochemical catalysts<sup>[43]</sup> for the hydrogen evolution reaction,<sup>[44]</sup> oxygen evolution/reduction reaction,<sup>[45]</sup> nitrogen reduction reaction,<sup>[46]</sup> and carbon dioxide reduction reaction.<sup>[47]</sup> As a result, ML is effective in promoting the development of metal–air batteries. A similar paradigm has been established with Li–S batteries for predicting the binding energies between lithium polysulfides and cathode hosts.<sup>[48]</sup> It should be noted that the choice of descriptors for the materials and the construction of ML models or algorithms are equally important in such ML studies.

Although physicochemical properties can, in principle, be calculated from the energies predicted by ML models for each component in a system or a reaction, it is more convenient to predict such terms of interest directly. For example, Jang and co-workers predicted the electrode potential of organic materials based on an ANN method.<sup>[49]</sup> The electron affinity, the highest occupied molecular orbital (HOMO) level, the lowest unoccupied molecular orbital (LUMO) level, HOMO–LUMO gap, and the number of oxygen and lithium atoms were chosen as the model features after careful engineering of the features. The ANN model is in good agreement with calculated results, with an averaged error of 3.54%. However, some input features of this model, such as the electronic affinity and HOMO/LUMO level, are still obtained from DFT calculations, which limits its scalability. Okamoto and Kubo constructed two regression models (Gaussian kernel ridge regression and gradient boosting regression) to predict the oxidation and reduction potentials of electrolyte additives.<sup>[50]</sup> The molecular features can be

obtained directly from the geometrical structures, including the number of atoms with the same coordination number, the number of five-membered and six-membered rings, and a flag to differ radical and nonradical molecules. The regression model with 22 features has been proved effective in predicting the redox potentials, especially the oxidation potentials, which is further rationalized by molecular orbital analyses.

Other than predicting system energy or its related parameters, ML is even more advantageous in determining physicochemical properties that are otherwise hard or expensive to obtain through either experiments or theoretical calculations, such as the ionic conductivity of solid-state electrolytes (SSEs), dielectric constant and viscosity of liquid electrolytes, and mechanical properties of solids. Taking the ionic conductivity of SSEs as an example, the apparent ionic conductivity of an SSE is easy to obtain experimentally but it is very sensitive to its synthesis conditions and testing methods. The intrinsic ionic conductivity of the materials, on the other hand, is hard to accurately measure through experiments because of the difficulty of separating the contribution from interfacial diffusivity. It is possible to calculate the intrinsic ionic conductivity through *ab initio* molecular dynamics (AIMD) simulations and mean square displacement (MSD) analysis. However, such simulations are generally computationally intensive. To circumvent such a dilemma, Reed and co-workers developed a data-driven logistic regression classification model based on experimental ionic conductivity data.<sup>[51]</sup> Out of 12 831 candidates, the model identified 21 promising structures with high lithium ionic conductivities. However, this ML model has 20 features but is trained only on 39 experimental data points. Considering the limitations of supervised learning models brought by the scarcity in available data on material properties, Mo, Ling, and co-workers developed an unsupervised ML model to discover new SSEs with promising ionic conductivity.<sup>[52]</sup> Li-containing compounds were clustered into seven groups based on their modified X-ray diffraction (mXRD) through unsupervised clustering methods, which helps to identify the common patterns in SSEs with high ionic conductivities. Such an unsupervised learning scheme discovered 16 new fast Li conductors with conductivities of  $10^{-4}$ – $10^{-1}$   $\text{Scm}^{-1}$ , which were further verified through AIMD simulations.

An alternative approach to break the limitations of conventional DFT and AIMD calculations is to develop highly accurate interatomic potentials. Different from the potentials adopted in classical MD simulations, ML is able to train from high-accuracy interatomic potentials obtained from DFT and AIMD calculations. The training process generally involves three key steps, building reference data, fingerprinting atomic environments, and establishing the correlation between the fingerprints and energies (Figure 5). The accuracy of the as-obtained ML potential is largely dependent on the selection of fingerprints, thus highlighting the irreplaceable role of capturing the local atomic environment of interesting structures. Zong et al. has achieved success in describing the pairwise, three-body, and many-body contributions to total energy through the terms derived from the change in bond length, material shape, and volume, respectively.<sup>[22]</sup> The fingerprints can subsequently be con-

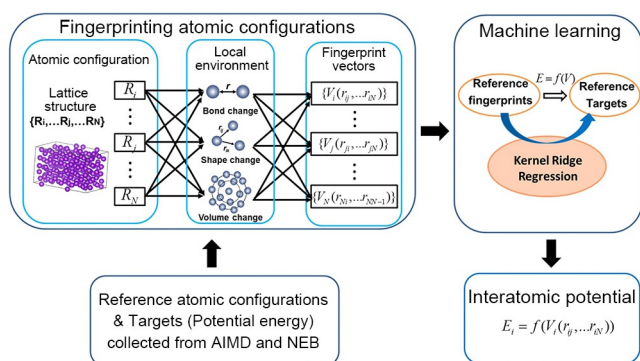


**Figure 5.** Developing machine-learning interatomic potentials. The development generally includes three parts: building reference data, fingerprinting atomic environments, and building the correlation between the fingerprints and energies to produce the interatomic potential. Reproduced with permission.<sup>[22]</sup> Copyright 2018, Springer Nature.

structured as long as those terms are well-defined. A variety of ML methods can then be chosen to describe the mapping between the fingerprints and atomic energies, from which interatomic potentials are generated. In addition to the above scenario, a deep-learning-based atomic potential has been recently developed, which generates the descriptors atomically and is independent of manual choices.<sup>[34]</sup>

ML-developed potentials have been widely applied in lithium battery studies, mainly for simulating the ionic transport in solid materials.<sup>[20,53,54]</sup> For example, Mueller and

co-workers developed a machine-learning interatomic potential based on moment tensor potentials to probe  $\text{Li}^+$  conduction in cathode coating materials (Figure 6).<sup>[53]</sup> Compared with SSEs, coating materials often possess a much lower ionic conductivity, which introduces great challenges to investigate the ionic transport by AIMD simulations. The machine-learning potential exhibits great superiority in high-temperature AIMD simulations both in terms of accuracy and computational efficiency (seven orders of magnitude faster than AIMD). The reduced prediction error of the Li ion diffusion barrier is mainly attributed to the improved statistics as a result of an extended simulation time and the prevention of phase transformation in high-temperature AIMD simulations.

The above example demonstrates the huge advantages and possibilities of ML intermolecular potentials in large time- or length-scale models. Apart from simulating the system energy or the ionic transport, ML interatomic potentials are also expected to help resolve other key challenges in rechargeable batteries: 1) probing the interfacial structures and ionic transport at grain boundaries or in amorphous materials, which often requires simulating a large system, 2) probing the electric double layer at the electrolyte-electrode interface, which strongly correlates to the electrochemical reactions and lithium ion (de-)solvation behaviors, 3) probing the solvation structure of electrolytes with complicated components or strong polarizations, the model size of which grows as the concentration of the electrolyte components decreases. Despite the great progress achieved in

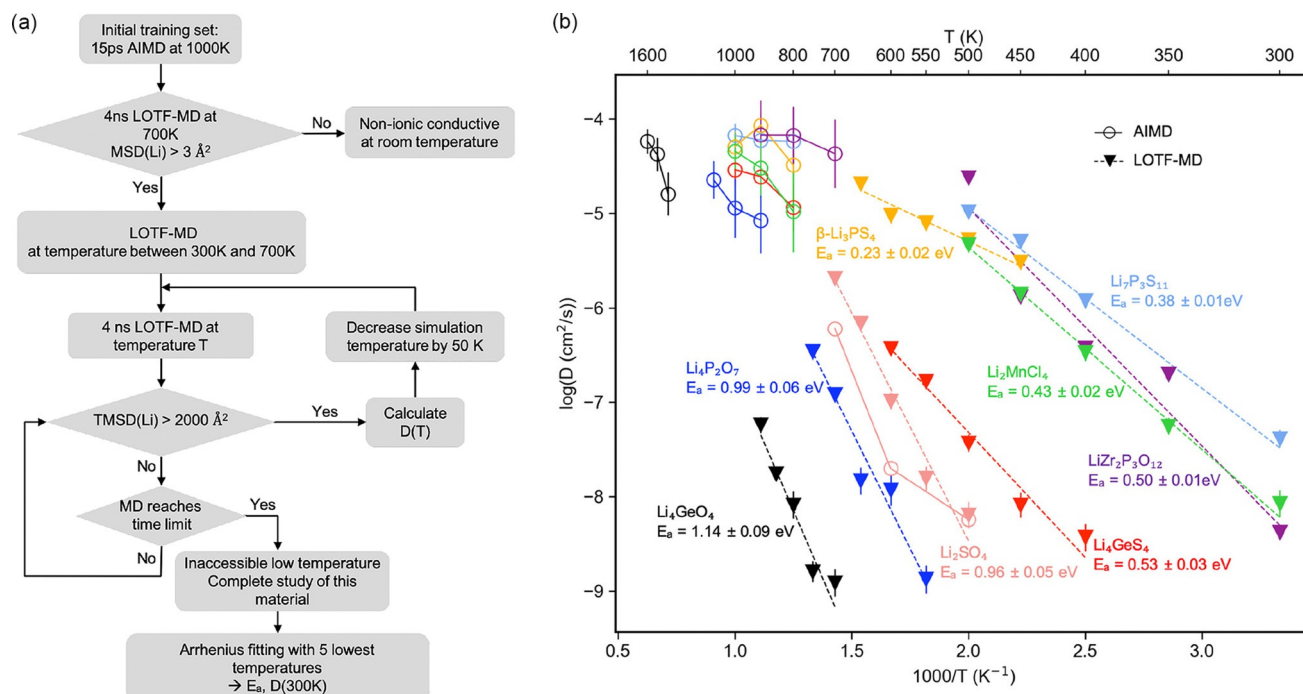


**Figure 6.** Machine learning intermolecular potential probes of ionic transport in solid materials. a) The flowchart of machine learning intermolecular potential in probing ionic conductivity. b) The comparison of diffusivities determined by AIMD simulations at high temperatures and LOTF-MD at intermediate temperatures on the Arrhenius plot. LOTF: „learning on the fly“, MSD: mean-square displacement, TMSD: total mean-square displacement, D: diffusivity, and E<sub>a</sub>: diffusion barrier. Reproduced with permission.<sup>[53]</sup> Copyright 2020, American Chemical Society.

polarizable force fields,<sup>[55]</sup> each treatment of polarization still requires several assumptions, which inevitably introduces limitations to the methods. ML intermolecular potential, on the other hand, brings new possibilities to tackle these complicated problems from an entirely different perspective.

### 3.2. PFM and FEM Simulations

Compared with atomic DFT calculations and MD simulations, mesoscale simulations can, in general, describe larger systems, successful applications of which have been well-established in lithium battery studies.<sup>[37,56]</sup> For example, PFM can accurately describe the microstructure evolution in batteries, such as dendritic growth, phase separation, coherency strain, and crack propagation. FEM, which is also applicable in macroscale simulations, is mainly adopted for analyzing electrochemical profiles, such as electric potential and ion concentration. The incorporation of ML into mesoscale simulations can also be categorized into two groups: learning from DFT or AIMD results to provide inputs for mesoscale simulations, as well as directly learning from mesoscale simulation results to establish a quantitative projection to experimental properties of interest. First, the reliability of mesoscale simulations largely depends on multiple physicochemical parameters and variants, such as free energy, dielectric constant, and diffusion coefficient. Some of these parameters can, in principle, be obtained through conventional DFT and MD simulations. However, the limitations of these microscale simulations start to become pronounced as the complexity of the systems increases. ML models can bridge this gap by extracting valuable information from DFT and AIMD results and encoding it as the input for mesoscale simulations. This method is, therefore, similar to developing ML intermolecular potentials.<sup>[57]</sup> For example, free energy density—a high-dimensional function of order parameters, composition, temperature, and etc.—has a significant impact on the reliability of phase field models but is typically hard to acquire with high accuracy from atomic-scale models or statistical mechanics. In an effort to circumvent this issue, Garikipati and co-workers developed analytically integrable deep neural networks (IDNNs) to represent the free energy density, which is then fed into phase field simulations to explore the phase stability of  $\text{Li}_x\text{CoO}_2$ .<sup>[57,58]</sup> Furthermore, although the variants of finite element models can in principle be obtained through experiments in most cases, the workload to construct a complete variant map of various parameters is actually overwhelming and not realistic. ML, on the other hand, eases the workload, as it has the capability to construct such maps based on information extracted from limited experimental results. For example, Wei and co-workers proposed a physics-driven ML-FEM algorithm and applied it to research on the deformation of Li metal, delivering highly accurate results with impressive efficiency.<sup>[59]</sup>

Apart from learning from microscale calculations to provide inputs for mesoscale simulations, ML can also directly learn from mesoscale simulations to obtain a quantitative relationship between various parameters and exper-

imental properties of interest,<sup>[60]</sup> the superiority of which is most prominent in the reduction of computational costs. For example, Dingreville and co-workers constructed a surrogate model for simulating the spinodal decomposition of a two-phase mixture by the combination of PFM simulations and a history-dependent ML approach, thereby reducing the computational time immensely at a minimal cost to the accuracy.<sup>[61]</sup> Such a ML-supported phase-field framework is also potentially applicable to PFM simulations of batteries, but requires further investigation. Other than reducing the computational cost, the advantage of ML has also been established in feature selection, as the most significant parameters can be easily identified through feature-importance analysis, a built-in function for many common ML algorithms. For example, Kriston et al. employed ML techniques to analyze 780 different numerically simulated thermal runaway events of LIBs and was able to identify five key clusters that distinguished LIBs with no or severe thermal runaway.<sup>[62]</sup> In general, ML-assisted PFM/FEM simulations have exhibited great potential, but are still in their infancy and further efforts are expected.

### 4. Mesoscale and Macroscale Experiments

Similar to theoretical microscale methods, ML has also demonstrated its superiority and potential in combination with experimental studies.<sup>[63]</sup> Its incorporation with experiments can be classified into three categories: assisting experimental result analysis (e.g. analyzing tomography data<sup>[64]</sup>), predicting key parameters from experimental data (e.g. battery lifespan prediction<sup>[65]</sup> and monitoring the state of health<sup>[66]</sup>), and optimizing experimental protocols (e.g. fast-charge protocol optimization<sup>[67]</sup>).

First, analyzing experimental results can sometimes present great challenges. For example, to ensure the maintenance of electrical conductivity in electrodes, the (de)attachment of electrode particles to or from the conductive matrix needs to be monitored, which can be hard to identify and segment (Figure 7).<sup>[64]</sup> Conventionally, the identification and segmentation of particles are achieved from reconstructed tomography data (Figure 7a) and require manual labeling, which is tedious and labour-intensive. Although traditional watershed and separation algorithms are capable of distinguishing de-attached particles, their limitations become pronounced when analyzing multiple fragments that have broken away from the same particle. To tackle this problem, Liu and co-workers developed a state-of-the-art mask regional convolutional neural network (Mask R-CNN), which successfully identified over 650 unique particles of different sizes, shapes, positions, and degrees of cracking based on a training set of manually labeled data (Figure 7b).<sup>[64]</sup> Similarly, Petrich et al. proposed a classification model to detect cracks in electrodes, from which a pair of particles resulted from breakage, image segmentation, or neither can be efficiently determined.<sup>[68]</sup> Besides tomography data, ML can potentially also be incorporated into the characterization of other images using a similar framework, such as optical microscopy, SEM, and TEM.



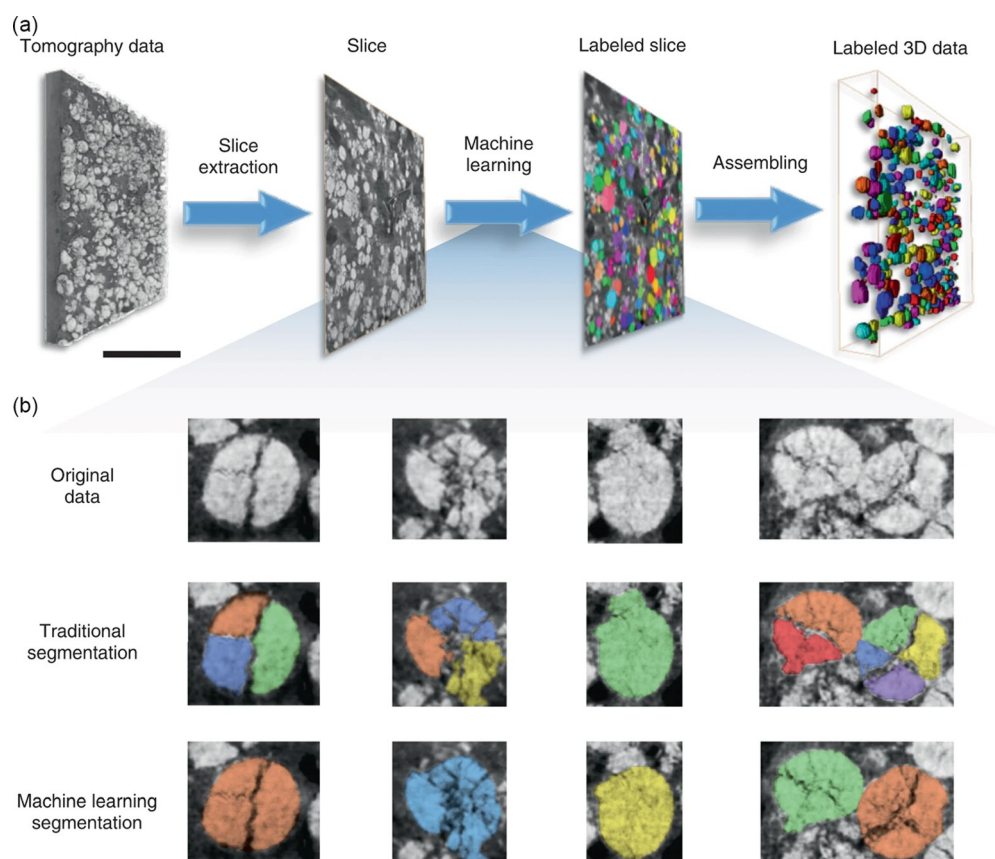


**Figure 7.** Machine-learning electrode particle segmentation. a) Workflow of the ML segmentation. b) Comparison of segmentations from traditional and ML approaches. Different colors denote different particles. The scale bar in (a) is 50  $\mu\text{m}$ . Reproduced with permission.<sup>[64]</sup> Copyright 2020, Springer Nature.

Another major application of machine learning in battery research lies in predicting electrochemical performance, as shown in Figure 8. Common variables quantifying the battery performance are usually chosen as the targets for prediction, such as the energy density, power density, lifespan, energy efficiency, high- or low-temperature performance etc. In addition, encouraged by the huge market potential of fast-charging batteries, optimization of the charging protocol becomes another target of great interest. Compared with determining the prediction target or response, more effort is required to craft the input features to describe a battery system. In general, the input feature can be classified into one of three categories based on the properties it aims to quantify: 1) the external environment, such as the temperature and stack pressure, 2) the components of the batteries, such as stoichiometry

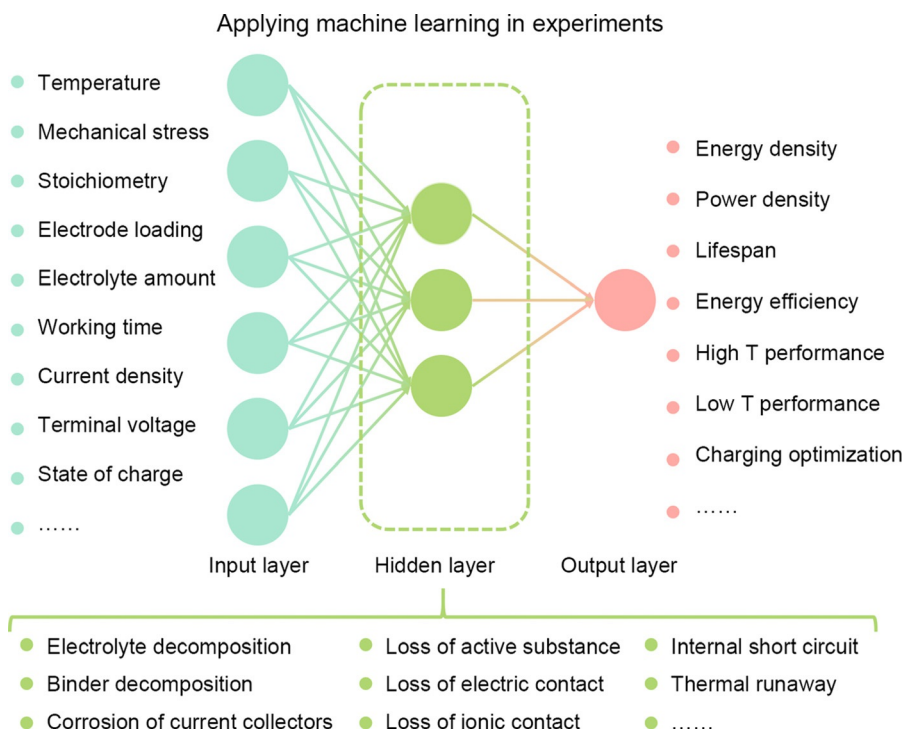


**Figure 8.** Correlating battery parameters and electrochemical performances through machine-learning approaches. T: temperature.

(cathode and anode active materials, charge/discharge reactions, and electrolyte recipes), electrode loading, and electrolyte amount, and 3) the working parameters of the battery, such as working time, charge/discharge current density, terminal voltage, and state-of-charge. Of course, not all the parameters are required, as a collection of batteries may share common features, such as environmental temperature and stack pressure. With the input features and output targets identified, great challenges still remain to develop proper models to describe their correlations. Such correlations are often complicated and strongly coupled with multiple physical processes and chemical reactions inside the battery, such as decomposition of the electrolyte, decomposition of the binder, corrosion of current collectors, loss of active substance, loss of electric contact, loss of ionic contact, internal short circuit, and thermal runaway. In the following, we present two examples to illustrate the transcendental progress made through applying machine learning to the prediction of battery performance.

Identifying the lifespan of a battery is one of the most crucial yet daunting challenges for the battery industry.

Measuring lifespan solely from experiments is impractical, as a cycling test over 10000 rounds at 1.0 C requires a run time of 833 days. Using ML to predict the battery lifetime based on the information from initial cycles is, therefore, a promising alternative to circumvent this obstacle. For example, Braatz and co-workers developed data-driven models that can accurately predict the cycle life of commercial lithium iron phosphate/graphite cells from early cycle data, without any prior knowledge of the degradation mechanisms.<sup>[69]</sup> The initial discharge capacity, charge time, temperature, and several other features extracted from the discharge voltage curves (such as the minimum, mean, variance, skewness, and kurtosis of the change in the discharge voltage curves between cycles 100 and 10) were adopted as the model inputs. Using information from only the first 100 cycles and trained by data from 124 cells with cycle lives ranging from 150 to 2300 under different charging procedures, the model was able to deliver a prediction error of 9.1 %. Furthermore, the model is able to classify cells into low- and high-lifetime groups using data from only the first 5 cycles, with only an impressive 4.9 % misclassification test error.

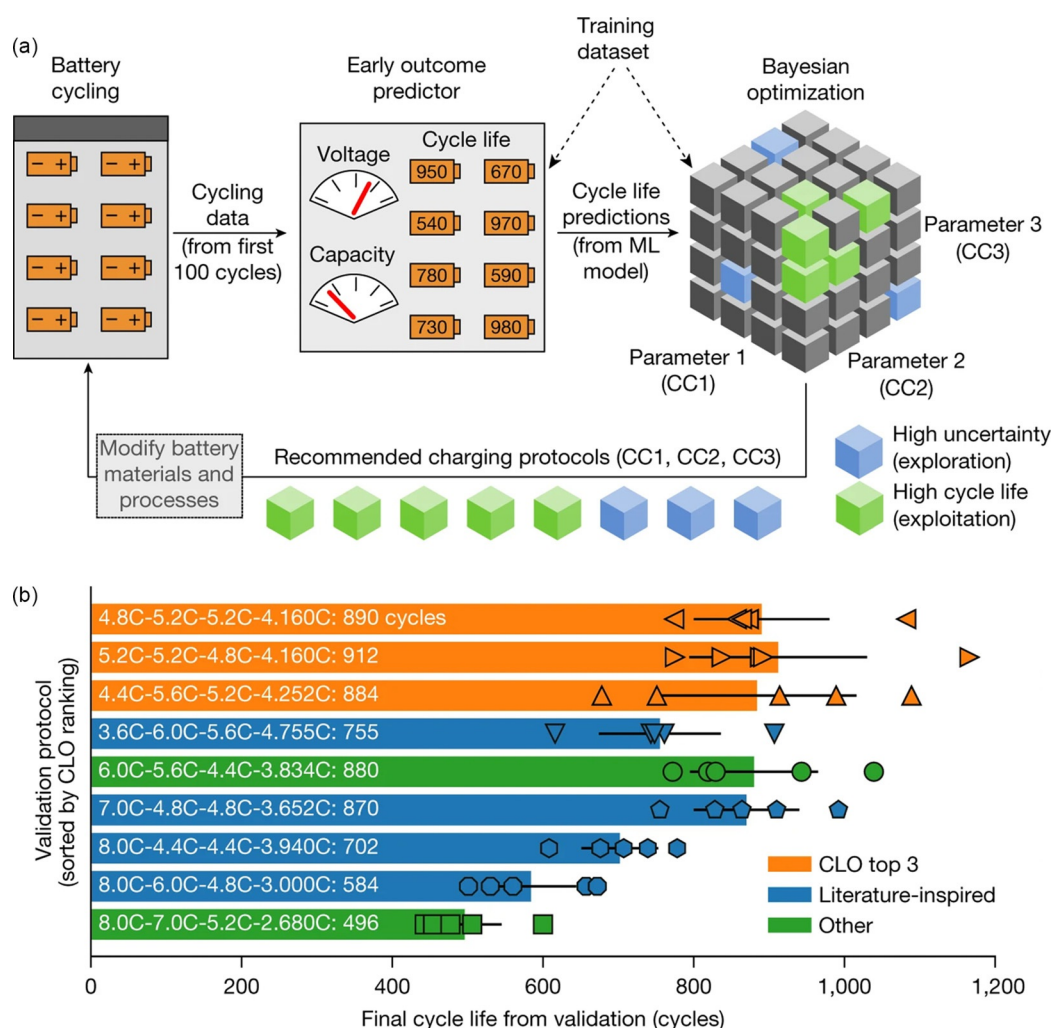


**Figure 9.** Optimizing fast-charge protocols for batteries through machine learning. a) The closed-loop optimization (CLO) system. b) The final cycle life from validation. The Bayesian approach demonstrates great advantages over the literature-inspired and other strategies. Reproduced with permission.<sup>[71]</sup> Copyright 2020, Springer Nature.

The cycle life of a battery is highly dependent on the charging protocols, and a state-of-charge from 0 to 80 % in ten minutes is demanded for practical use.<sup>[70]</sup> However, both large parameter space and high sampling variability increase the number of experiments required, thus reducing the feasibility of protocol optimization through only experiments. To overcome this hurdle, Chueh and co-workers developed a Bayesian optimization algorithm to optimize a parameter space specifying the current and voltage profiles of six-step, ten-minute fast-charging protocols for maximizing battery cycle life (Figure 9a).<sup>[71]</sup> The battery lifespan can be predicted from information from the first 100 cycles through ML models, with outputs subsequently sent to the Bayesian optimization algorithm. The algorithm then attempts to optimize the charging parameters CC1, CC2, and CC3, which represent the charging rates of the first, second, and third stages, respectively. The length of experiments can firstly be reduced by the adoption of an early prediction ML model, as it predicts the cycle life based on data from only the first 100 cycles. In addition, the number of experiments can be further decreased by the Bayesian optimization algorithm, which balances the exploration and exploitation to probe the parameter space of charging protocols efficiently. As a result, this novel method is capable of rapidly identifying high-cycle-life charging protocols among 224 candidates in 16 days, which is over 30 times faster than conventional exhaustive approaches. More importantly, the optimized protocol identified by the ML model outperforms protocols inspired by previous literature reports (895 vs. 728 cycles on average; Figure 9b).

## 5. Summary and Outlook

As discussed above, emerging machine-learning methods are generating a revolution in research. Experimental, theoretical, and data tools have become three indispensable and correlating parts in battery manufacturing, management, and monitoring (Figure 10). An outlook on future applications of machine learning in rechargeable batteries is discussed in the following paragraphs.

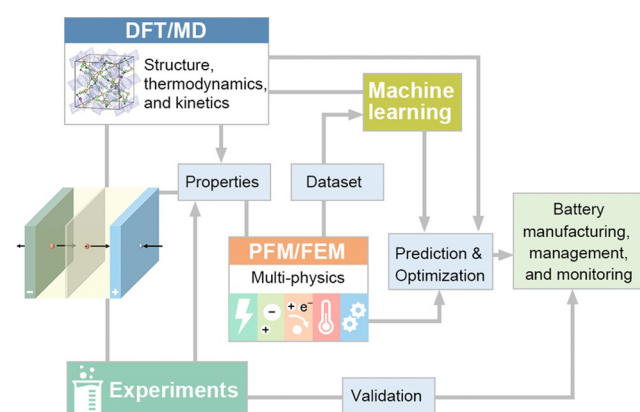


**Figure 10.** Coupling multiscale calculations, experiments, and machine learning in battery studies, including manufacturing, management, and monitoring.

First, machine learning accelerates the development of powerful theoretical tools, such as advanced functionals for DFT calculations, efficient potentials for MD simulations, and novel approaches to solve multiscale physical equations. It is expected to enable high-accuracy atomic simulations for large systems, which makes probing complicated geometrical structures, charge distribution, thermal and kinetic stabilities, and ionic diffusivity at interfaces or in amorphous phases possible. A deeper fundamental understanding of the working mechanisms and material evolution schemes during electrochemical reactions can, therefore, be obtained, thereby assisting the search and design of novel materials and battery recipes.

Second, human intuition is very powerful in extracting knowledge from successful trial-and-error experiments, whereas ML-based data mining methods are able to excavate valuable information behind numerous failed experiments.<sup>[17]</sup> Specifically, data-driven methods exhibit a great potential for monitoring the working status of batteries and forecasting their cycle lives.

Third, the large parameter spaces and high sampling variability have led to parameter optimization for battery manufacturing and management being extremely challenging, whereas ML-based models can mitigate these obstacles through rational algorithm design. For example, ML models can be applied to optimize the fast-charge protocol and electrolyte component ratio. Bayesian algorithm-based ML models have been shown to significantly reduce the parameter space and, consequently, the number of experiments required. Furthermore, this approach can also be extended to optimize the synthetic conditions of battery materials and even propose alternative strategies for material design based on a quantitative structure–property relationship.

Lastly, although the value and impact of machine-learning and artificial intelligence methods in battery research continue to grow, human knowledge remains an indispensable, and perhaps even the most important, part. The choice of model features, as well as the development of training algorithms, are still highly dependent on human judgement and the knowledge of the experts. Nevertheless, we believe that ML can bring new vitality to conventional theoretical and experimental methods and that the revolutionary data-driven research holds promise to accelerate the development of future rechargeable batteries.

## Acknowledgements

This work was supported by the National Natural Science Foundation of China (21825501), Beijing Municipal Natural Science Foundation (Z20J00043), and Grant 2020GQG1006 from the Guoqiang Institute at Tsinghua University. X.C. appreciates support from the Shuimu Tsinghua Scholar Program of Tsinghua University and the Project funded by the China Postdoctoral Science Foundation (2021TQ0161 and 2021M691709).



## Conflict of Interest

The authors declare no conflict of interest.

- [1] M. Armand, J. M. Tarascon, *Nature* **2008**, *451*, 652–657.
- [2] D. Larcher, J. M. Tarascon, *Nat. Chem.* **2015**, *7*, 19–29.
- [3] M. Winter, B. Barnett, K. Xu, *Chem. Rev.* **2018**, *118*, 11433–11456.
- [4] D. Lin, Y. Liu, Y. Cui, *Nat. Nanotechnol.* **2017**, *12*, 194–206; H. J. Peng, J. Q. Huang, Q. Zhang, *Chem. Soc. Rev.* **2017**, *46*, 5237–5288.
- [5] X.-B. Cheng, R. Zhang, C.-Z. Zhao, Q. Zhang, *Chem. Rev.* **2017**, *117*, 10403–10473.
- [6] X. Chen, T. Hou, K. A. Persson, Q. Zhang, *Mater. Today* **2019**, *22*, 142–158.
- [7] Y. Cao, M. Li, J. Lu, J. Liu, K. Amine, *Nat. Nanotechnol.* **2019**, *14*, 200–207.
- [8] X. Zhang, Y. Yang, Z. Zhou, *Chem. Soc. Rev.* **2020**, *49*, 3040–3071.
- [9] S. Wei, S. Choudhury, Z. Tu, K. Zhang, L. A. Archer, *Acc. Chem. Res.* **2018**, *51*, 80–88; X. Zhang, A. Wang, X. Liu, J. Luo, *Acc. Chem. Res.* **2019**, *52*, 3223–3232; X. Gao, Y.-N. Zhou, D. Han, J. Zhou, D. Zhou, W. Tang, J. B. Goodenough, *Joule* **2020**, *4*, 1864–1879.
- [10] X. Chen, Q. Zhang, *Acc. Chem. Res.* **2020**, *53*, 1992–2002.
- [11] A. A. Franco, A. Rucci, D. Brandell, C. Frayret, M. Gaberscek, P. Jankowski, P. Johansson, *Chem. Rev.* **2019**, *119*, 4569–4627; A. Van der Ven, Z. Deng, S. Banerjee, S. P. Ong, *Chem. Rev.* **2020**, *120*, 6977–7019; M. S. Islam, C. A. Fisher, *Chem. Soc. Rev.* **2014**, *43*, 185–204.
- [12] X. Chen, X.-Q. Zhang, H.-R. Li, Q. Zhang, *Batteries Supercaps* **2019**, *2*, 128–131.
- [13] O. Borodin, X. Ren, J. Vatamanu, A. von Wald Cresce, J. Knap, K. Xu, *Acc. Chem. Res.* **2017**, *50*, 2886–2894.
- [14] X. Chen, H.-R. Li, X. Shen, Q. Zhang, *Angew. Chem. Int. Ed.* **2018**, *57*, 16643–16647; *Angew. Chem.* **2018**, *130*, 16885–16889; X. Chen, X. Shen, B. Li, H. J. Peng, X. B. Cheng, B. Q. Li, X. Q. Zhang, J. Q. Huang, Q. Zhang, *Angew. Chem. Int. Ed.* **2018**, *57*, 734–737; *Angew. Chem.* **2018**, *130*, 742–745.
- [15] A. M. Nolan, Y. Zhu, X. He, Q. Bai, Y. Mo, *Joule* **2018**, *2*, 2016–2046; Z.-H. Fu, X. Chen, C.-Z. Zhao, H. Yuan, R. Zhang, X. Shen, X.-X. Ma, Y. Lu, Q.-B. Liu, L.-Z. Fan, Q. Zhang, *Energy Fuels* **2021**, *35*, 10210–10218.
- [16] R. Pollice, G. dos Passos Gomes, M. Aldeghi, R. J. Hickman, M. Krenn, C. Lavigne, M. Lindner-D'Addario, A. Nigam, C. T. Ser, Z. Yao, A. Aspuru-Guzik, *Acc. Chem. Res.* **2021**, *54*, 849–860; D. Krishnamurthy, H. Weiland, A. Barati Farimani, E. Antonio, J. Green, V. Viswanathan, *ACS Energy Lett.* **2019**, *4*, 187–191; J.-P. Correa-Baena, K. Hippalgaonkar, J. van Duren, S. Jaffer, V. R. Chandrasekhar, V. Stevanovic, C. Wadia, S. Guha, T. Buonassisi, *Joule* **2018**, *2*, 1410–1420; S. M. Moosavi, K. M. Jablonka, B. Smit, *J. Am. Chem. Soc.* **2020**, *142*, 20273–20287; O. A. von Lilienfeld, K.-R. Müller, A. Tkatchenko, *Nat. Rev. Chem.* **2020**, *4*, 347–358; R. Batra, L. Song, R. Ramprasad, *Nat. Rev. Mater.* **2021**, *6*, 655–678; D. M. Wilkins, A. Grisafi, Y. Yang, K. U. Lao, R. A. DiStasio, M. Ceriotti, *Proc. Natl. Acad. Sci. USA* **2019**, *116*, 3401–3406; D. T. Ahneman, J. G. Estrada, S. Lin, S. D. Dreher, A. G. Doyle, *Science* **2018**, *360*, 186–190; M. Meuwly, *Chem. Rev.* **2021**, <https://doi.org/10.1021/acs.chemrev.1c00033>.
- [17] P. Raccuglia, K. C. Elbert, P. D. F. Adler, C. Falk, M. B. Wenny, A. Mollo, M. Zeller, S. A. Friedler, J. Schrier, A. J. Norquist, *Nature* **2016**, *533*, 73–76.
- [18] S. Dick, M. Fernandez-Serra, *Nat. Commun.* **2020**, *11*, 3509.
- [19] P. Borlido, J. Schmidt, A. W. Huran, F. Tran, M. A. L. Marques, S. Botti, *npj Comput. Mater.* **2020**, *6*, 96.
- [20] N. Xu, Y. Shi, Y. He, Q. Shao, *J. Phys. Chem. C* **2020**, *124*, 16278–16288.
- [21] P. Yoo, M. Sakano, S. Desai, M. M. Islam, P. Liao, A. Strachan, *npj Comput. Mater.* **2021**, *7*, 9; C. W. Rosenbrock, K. Gubaev, A. V. Shapeev, L. B. Pártay, N. Bernstein, G. Csányi, G. L. W. Hart, *npj Comput. Mater.* **2021**, *7*, 24; S. Manzhos, T. Carrington, *Chem. Rev.* **2021**, <https://doi.org/10.1021/acs.chemrev.0c00665>; P. Friederich, F. Häse, J. Proppe, A. Aspuru-Guzik, *Nat. Mater.* **2021**, *20*, 750–761.
- [22] H. Zong, G. Pilania, X. Ding, G. J. Ackland, T. Lookman, *npj Comput. Mater.* **2018**, *4*, 48.
- [23] K. T. Butler, D. W. Davies, H. Cartwright, O. Isayev, A. Walsh, *Nature* **2018**, *559*, 547–555.
- [24] B. Qiao, S. Mohapatra, J. Lopez, G. M. Leverick, R. Tatara, Y. Shibuya, Y. Jiang, A. France-Lanord, J. C. Grossman, R. Gómez-Bombarelli, J. A. Johnson, Y. Shao-Horn, *ACS Cent. Sci.* **2020**, *6*, 1115–1128.
- [25] X. Yang, Y. Wang, R. Byrne, G. Schneider, S. Yang, *Chem. Rev.* **2019**, *119*, 10520–10594.
- [26] S. Ekins, A. C. Puhl, K. M. Zorn, T. R. Lane, D. P. Russo, J. J. Klein, A. J. Hickey, A. M. Clark, *Nat. Mater.* **2019**, *18*, 435–441.
- [27] Z. Ahmad, T. Xie, C. Maheshwari, J. C. Grossman, V. Viswanathan, *ACS Cent. Sci.* **2018**, *4*, 996–1006; Y. Liu, B. Guo, X. Zou, Y. Li, S. Shi, *Energy Storage Mater.* **2020**, *31*, 434–450; J.-X. Huang, G. Csányi, J.-B. Zhao, J. Cheng, V. L. Deringer, *J. Mater. Chem. A* **2019**, *7*, 19070–19080; B. Liu, J. Yang, H. Yang, C. Ye, Y. Mao, J. Wang, S. Shi, J. Yang, W. Zhang, *J. Mater. Chem. A* **2019**, *7*, 19961–19969; K. Suzuki, K. Ohura, A. Seko, Y. Iwamizu, G. Zhao, M. Hirayama, I. Tanaka, R. Kanno, *J. Mater. Chem. A* **2020**, *8*, 11582–11588.
- [28] Y. Kang, L. Li, B. Li, *J. Energy Chem.* **2021**, *54*, 72–88.
- [29] K. M. Jablonka, D. Ongari, S. M. Moosavi, B. Smit, *Chem. Rev.* **2020**, *120*, 8066–8129.
- [30] P. M. Pflüger, F. Glorius, *Angew. Chem. Int. Ed.* **2020**, *59*, 18860–18865; *Angew. Chem.* **2020**, *132*, 19020–19025; B. Sanchez-Lengeling, A. Aspuru-Guzik, *Science* **2018**, *361*, 360–365.
- [31] C. Chen, Y. Zuo, W. Ye, X. Li, Z. Deng, S. P. Ong, *Adv. Energy Mater.* **2020**, *10*, 1903242; J. Graser, S. K. Kauwe, T. D. Sparks, *Chem. Mater.* **2018**, *30*, 3601–3612; T. Wang, C. Zhang, H. Snoussi, G. Zhang, *Adv. Funct. Mater.* **2020**, *30*, 1906041.
- [32] K. Xu, *Chem. Rev.* **2004**, *104*, 4303–4417; K. Xu, *Chem. Rev.* **2014**, *114*, 11503–11618.
- [33] D. Lu, H. Wang, M. Chen, L. Lin, R. Car, W. Jia, L. Zhang, *Comput. Phys. Commun.* **2021**, *259*, 107624.
- [34] H. Wang, L. Zhang, J. Han, *Comput. Phys. Commun.* **2018**, *228*, 178–184.
- [35] T. Z. Hou, W. T. Xu, X. Chen, H. J. Peng, J. Q. Huang, Q. Zhang, *Angew. Chem. Int. Ed.* **2017**, *56*, 8178–8182; *Angew. Chem.* **2017**, *129*, 8290–8294; R. Zhang, X. Chen, X. Shen, X.-Q. Zhang, X.-R. Chen, X.-B. Cheng, C. Yan, C.-Z. Zhao, Q. Zhang, *Joule* **2018**, *2*, 764–777; X. Chen, T.-Z. Hou, B. Li, C. Yan, L. Zhu, C. Guan, X.-B. Cheng, H.-J. Peng, J.-Q. Huang, Q. Zhang, *Energy Storage Mater.* **2017**, *8*, 194–201.
- [36] X. Chen, X. Shen, T.-Z. Hou, R. Zhang, H.-J. Peng, Q. Zhang, *Chem* **2020**, *6*, 2242–2256.
- [37] R. Zhang, X. Shen, X.-B. Cheng, Q. Zhang, *Energy Storage Mater.* **2019**, *23*, 556–565.
- [38] L. Kong, X. Chen, B. Q. Li, H. J. Peng, J. Q. Huang, J. Xie, Q. Zhang, *Adv. Mater.* **2018**, *30*, 1705219; H. J. Peng, G. Zhang, X. Chen, Z. W. Zhang, W. T. Xu, J. Q. Huang, Q. Zhang, *Angew. Chem. Int. Ed.* **2016**, *55*, 12990–12995; *Angew. Chem.* **2016**, *128*, 13184–13189; X. Tao, J. Wang, C. Liu, H. Wang, H. Yao, G. Zheng, Z. W. Seh, Q. Cai, W. Li, G. Zhou, C. Zu, Y. Cui, *Nat. Commun.* **2016**, *7*, 11203; G. Zhou, H. Tian, Y. Jin, X. Tao, B. Liu, R. Zhang, Z. W. Seh, D. Zhuo, Y. Liu, J. Sun, J. Zhao, C. Zu, D. S. Wu, Q. Zhang, Y. Cui, *Proc. Natl. Acad. Sci. USA* **2017**, *114*, 840–845; L. Peng, Z. Wei, C. Wan, J. Li, Z. Chen, D. Zhu, D.

- Baumann, H. Liu, C. S. Allen, X. Xu, A. I. Kirkland, I. Shakir, Z. Almutairi, S. Tolbert, B. Dunn, Y. Huang, P. Sautet, X. Duan, *Nat. Catal.* **2020**, *3*, 762–770; X. Chen, H.-J. Peng, R. Zhang, T.-Z. Hou, J.-Q. Huang, B. Li, Q. Zhang, *ACS Energy Lett.* **2017**, *2*, 795–801.
- [39] K. Yoshida, M. Nakamura, Y. Kazue, N. Tachikawa, S. Tsuzuki, S. Seki, K. Dokko, M. Watanabe, *J. Am. Chem. Soc.* **2011**, *133*, 13121–13129; J. Qian, W. A. Henderson, W. Xu, P. Bhattacharya, M. Engelhard, O. Borodin, J.-G. Zhang, *Nat. Commun.* **2015**, *6*, 6362.
- [40] Y. Wang, W. D. Richards, S. P. Ong, L. J. Miara, J. C. Kim, Y. Mo, G. Ceder, *Nat. Mater.* **2015**, *14*, 1026–1031; X. He, Y. Zhu, Y. Mo, *Nat. Commun.* **2017**, *8*, 15893; Y. Mo, S. P. Ong, G. Ceder, *Chem. Mater.* **2012**, *24*, 15–17.
- [41] J. Sun, A. Ruzsinszky, J. P. Perdew, *Phys. Rev. Lett.* **2015**, *115*, 036402.
- [42] M. Yu, S. Yang, C. Wu, N. Marom, *npj Comput. Mater.* **2020**, *6*, 180.
- [43] M. Andersen, K. Reuter, *Acc. Chem. Res.* **2021**, *54*, 2741–2749.
- [44] H. Li, S. Xu, M. Wang, Z. Chen, F. Ji, K. Cheng, Z. Gao, Z. Ding, W. Yang, *J. Mater. Chem. A* **2020**, *8*, 17987–17997.
- [45] Y. Sun, H. Liao, J. Wang, B. Chen, S. Sun, S. J. H. Ong, S. Xi, C. Diaoy, Y. Du, J.-O. Wang, M. B. H. Breese, S. Li, H. Zhang, Z. J. Xu, *Nat. Catal.* **2020**, *3*, 554–563; L. Wu, T. Guo, T. Li, *iSci.* **2021**, *24*, 102398; S. Lin, H. Xu, Y. Wang, X. C. Zeng, Z. Chen, *J. Mater. Chem. A* **2020**, *8*, 5663–5670; C. Deng, Y. Su, F. Li, W. Shen, Z. Chen, Q. Tang, *J. Mater. Chem. A* **2020**, *8*, 24563–24571; J. Kang, S. H. Noh, J. Hwang, H. Chun, H. Kim, B. Han, *Phys. Chem. Chem. Phys.* **2018**, *20*, 24539–24544; X. Zhu, J. Yan, M. Gu, T. Liu, Y. Dai, Y. Gu, Y. Li, *J. Phys. Chem. Lett.* **2019**, *10*, 7760–7766; L. Wu, T. Guo, T. Li, *J. Mater. Chem. A* **2020**, *8*, 19290–19299.
- [46] M. Zafari, D. Kumar, M. Umer, K. S. Kim, *J. Mater. Chem. A* **2020**, *8*, 5209–5216; G. Zheng, Y. Li, X. Qian, G. Yao, Z. Tian, X. Zhang, L. Chen, *ACS Appl. Mater. Interfaces* **2021**, *13*, 16336–16344.
- [47] A. Chen, X. Zhang, L. Chen, S. Yao, Z. Zhou, *J. Phys. Chem. C* **2020**, *124*, 22471–22478; Z. Yang, W. Gao, Q. Jiang, *J. Mater. Chem. A* **2020**, *8*, 17507–17515.
- [48] H. Zhang, Z. Wang, J. Ren, J. Liu, J. Li, *Energy Storage Mater.* **2021**, *35*, 88–98.
- [49] O. Allam, B. W. Cho, K. C. Kim, S. S. Jang, *RSC Adv.* **2018**, *8*, 39414–39420.
- [50] Y. Okamoto, Y. Kubo, *ACS Omega* **2018**, *3*, 7868–7874.
- [51] A. D. Sendek, Q. Yang, E. D. Cubuk, K.-A. N. Duerloo, Y. Cui, E. J. Reed, *Energy Environ. Sci.* **2017**, *10*, 306–320.
- [52] Y. Zhang, X. He, Z. Chen, Q. Bai, A. M. Nolan, C. A. Roberts, D. Banerjee, T. Matsunaga, Y. Mo, C. Ling, *Nat. Commun.* **2019**, *10*, 5260.
- [53] C. Wang, K. Aoyagi, P. Wisesa, T. Mueller, *Chem. Mater.* **2020**, *32*, 3741–3752.
- [54] W. Li, Y. Ando, E. Minamitani, S. Watanabe, *J. Chem. Phys.* **2017**, *147*, 214106; V. L. Deringer, *J. Phys. Energy* **2020**, *2*, 041003; K. Miwa, R. Asahi, *Phys. Rev. Mater.* **2018**, *2*, 105404; K. Miwa, R. Asahi, *Solid State Ionics* **2021**, *361*, 115567.
- [55] D. Bedrov, J.-P. Piquemal, O. Borodin, A. D. MacKerell, B. Roux, C. Schröder, *Chem. Rev.* **2019**, *119*, 7940–7995.
- [56] X. Shen, R. Zhang, X. Chen, X.-B. Cheng, X. Li, Q. Zhang, *Adv. Energy Mater.* **2020**, *10*, 1903645; X. Shen, R. Zhang, P. Shi, X. Chen, Q. Zhang, *Adv. Energy Mater.* **2021**, *11*, 2003416; M. Z. Bazant, *Acc. Chem. Res.* **2013**, *46*, 1144–1160.
- [57] G. H. Teichert, S. Das, M. Aykol, C. Gopal, V. Gavini, K. Garikipati, *arXiv* **2021**, <https://arxiv.org/abs/2104.08318v2>.
- [58] G. H. Teichert, A. R. Natarajan, A. Van der Ven, K. Garikipati, *Comput. Methods Appl. M* **2019**, *353*, 201–216.
- [59] J. Wen, Q. Zou, Y. Wei, *J. Mech. Phys. Solids J. Mech. Phys. Solids* **2021**, *153*, 104481.
- [60] O. Kononenko, I. Kononenko, *arXiv* **2018**, <https://arxiv.org/abs/1801.07337>.
- [61] D. Montes de Oca Zapiain, J. A. Stewart, R. Dingreville, *npj Comput. Mater.* **2021**, *7*, 3.
- [62] A. Kriston, A. Podias, I. Adanouj, A. Pfrang, *J. Electrochem. Soc.* **2020**, *167*, 090555.
- [63] S. R. Hashemi, A. Bahadoran Baghbadorani, R. Esmaeeli, A. Mahajan, S. Farhad, *Int. J. Energy Res.* **2021**, *45*, 5747–5765; A. Garg, S. Singh, W. Li, L. Gao, X. Cui, C.-T. Wang, X. Peng, N. Rajasekar, *Int. J. Energy Res.* **2020**, *44*, 9513–9526; B.-R. Chen, M. R. Kunz, T. R. Tanim, E. J. Dufek, *Cell Rep. Phys. Sci.* **2021**, *2*, 100352; D. Zhou, W. Zheng, P. Fu, X. Pan, *J. Power Sources* **2020**, *451*, 227713.
- [64] Z. Jiang, J. Li, Y. Yang, L. Mu, C. Wei, X. Yu, P. Pianetta, K. Zhao, P. Cloetens, F. Lin, Y. Liu, *Nat. Commun.* **2020**, *11*, 2310.
- [65] Y. Zhang, Q. Tang, Y. Zhang, J. Wang, U. Stimming, A. A. Lee, *Nat. Commun.* **2020**, *11*, 1706; P. Fermín-Cueto, E. McTurk, M. Allerhand, E. Medina-Lopez, M. F. Anjos, J. Sylvester, G. dos Reis, *Energy AI* **2020**, *1*, 100006; Z. Fei, F. Yang, K.-L. Tsui, L. Li, Z. Zhang, *Energy* **2021**, *225*, 120205.
- [66] D. Roman, S. Saxena, V. Robu, M. Pecht, D. Flynn, *Nat. Mach. Intell.* **2021**, *3*, 447–456; M.-F. Ng, J. Zhao, Q. Yan, G. J. Conduit, Z. W. Seh, *Nat. Mach. Intell.* **2020**, *2*, 161–170.
- [67] Y. Yang, *Appl. Energy* **2021**, *292*, 116897.
- [68] L. Petrich, D. Westhoff, J. Feinauer, D. P. Finegan, S. R. Daemi, P. R. Shearing, V. Schmidt, *Comput. Mater. Sci.* **2017**, *136*, 297–305.
- [69] K. A. Severson, P. M. Attia, N. Jin, N. Perkins, B. Jiang, Z. Yang, M. H. Chen, M. Aykol, P. K. Herring, D. Fraggadakis, M. Z. Bazant, S. J. Harris, W. C. Chueh, R. D. Braatz, *Nat. Energy* **2019**, *4*, 383–391.
- [70] Y. Liu, Y. Zhu, Y. Cui, *Nat. Energy* **2019**, *4*, 540–550.
- [71] P. M. Attia, A. Grover, N. Jin, K. A. Severson, T. M. Markov, Y.-H. Liao, M. H. Chen, B. Cheong, N. Perkins, Z. Yang, P. K. Herring, M. Aykol, S. J. Harris, R. D. Braatz, S. Ermon, W. C. Chueh, *Nature* **2020**, *578*, 397–402.

Manuskript erhalten: 2. Juni 2021

Akzeptierte Fassung online: 30. Juni 2021

Endgültige Fassung online: 20. August 2021